

Canopy Temperature as Indicator of Water Stress: Image analysis of grapevine canopies.

Yann Guisard^{1*}, Jeremy P.M. Whish², Geoffrey R. Scollary³

Abstract

Canopy temperature has been proposed in field crop and horticulture industries as an indicator of plant water stress, using absolute and/or relative indices. Infrared thermographers are now available at relatively low cost but integrate exposed and shaded leaves in their fields of view. Shaded leaves have a different temperature distribution than exposed leaves. Separation of the exposed and shaded fractions in thermal datasets is critical for subsequent analysis, particularly when canopies display a spherical leaf angle distribution. Various classification and warping algorithms available in the image analysis software ENVI 4.2 were assessed to separate the exposed and shaded fraction of field grown grapevines canopies (*Vitis vinifera* L. cv Cabernet Sauvignon). The Parallelepiped algorithm with User Defined mix of standard deviation and the polynomial (1st degree) warping algorithm are recommended for the classification and warping of visible images respectively. The mean temperature of the various fractions was significantly different from each other as well as from the combined regions' mean. The Regions of Interests (ROI) defined to classify the images displayed good separability, suggesting the possible automation of the process. An analysis of Red, Green and Blue (RGB) bands and Hue, Saturation and Value (HSV) transformed bands of the visible images showed that HSV images were less sensitive than RGB images to the factors affecting the capture of data by the camera, and should therefore be preferred. These results did not however support the suggestion that spectral libraries or endmember collections may be used to automate the classification procedure. A calibration methodology involving points of known RGB and/or HSV is proposed to reduce the effect of the various factors is discussed for future automated procedures.

Key Words

Infrared thermography, image analysis, image classification, warping, endmember collection, spectral libraries, spherical leaf angle distribution.

Introduction

Canopy temperature as an indicator of plant water stress and its possible use in irrigation scheduling was proposed several decades ago, but required cumbersome and impractical instruments (Tanner, 1963).

The subsequent four decades saw the development of various indices based partially or entirely on canopy temperature measured remotely by infrared thermometry, infrared thermography or fine copper thermocouples. Such indices included an early proposal of the Stress Day Index (Hiler *et al.*, 1974), the

^{1*} Corresponding author, National Wine and Grape Industry Centre - Charles Sturt University, PO Box 883, Orange, NSW, 2800, Australia. yguisard@csu.edu.au

² CSIRO Sustainable Ecosystems, Agricultural Production Systems Research Unit.

³ Retired Director, National Wine and Grape Industry Centre.

Stress Degree Day (Idso *et al.*, 1977), the Temperature Stress Day (Blad *et al.*, 1981), the Crop Water Stress Index (Idso *et al.*, 1981) and more recently the Canopy Stress Index (Rodriguez *et al.*, 2005).

The development of relative indices was shown to have a better mechanistic foundation and the ability to differentiate between plant and non-plant material. Such indices include the Water Deficit Index (Moran *et al.*, 1994), Jones's Index (Jones, 1999) as well as a re-formulation of the Crop Water Stress Index by Jones (1999). Various drought monitoring and plant health indices have been reported in the literature, but are used at large scales, and are unsuitable for block irrigation scheduling (Bhuiyan, 2004; Kogan, 1995; Singh *et al.*, 2003).

The recent interest shown in using plant canopy temperature as an irrigation scheduling tool is justified by the dramatic reduction in instrumentation cost observed over the last few years. Jones (2004) reviewed the advantages and pitfalls of plant based irrigation scheduling, warning of the requirement for calibration (possibly through the use of relative indices) for better interpretation of the raw measures.

Recent studies on grapevines (*Vitis vinifera* L.) have demonstrated the capacity of Jones' I_g and I_{CWSI} indices (Jones, 1999) to successfully differentiate between fully irrigated and several deficit irrigation treatments (Fuentes *et al.*, 2005; Jones *et al.*, 2002; Leinonen and Jones, 2004; Moller *et al.*, 2007; Stoll and Jones, 2005) when canopies display a planar leaf angle distribution. Various methodologies were used to exclude non-tissue material from the computation of the indices, including considerable thermal image analyses from Cohen *et al.*, (2005), but only Leinonen and Jones (2004) proposed to separate the exposed from the shaded fractions from the canopy. These authors showed a significant difference between the distribution composition of the two fractions, and the associated improvement in the interpretability of the indices when the fractions were separated from one another.

If thermal indices are to be used in vineyards and orchards displaying spherical leaf angle distributions, discrimination between canopy exposure fractions is critically important. As pointed out by Jones (2002) using the conclusions drawn from Fuchs (1990), the variability of the index may indeed be a better indicator for irrigation requirement than its mean value. As the sampling time approaches solar noon and the number of shaded pixels increases, the impact of the various fractions on indices computation is likely to increase. It is therefore proposed that the separation of the exposed and shaded fractions of grapevine canopies be carried out using analysis of visible images, prior to integration with thermal data to study the temperature distribution of the various fractions. The present work is part of a larger project focussing on grapevine canopies displaying a spherical leaf angle distribution (Guisard, 2008) and will address the following questions: (1) can the separation of the exposed and shaded fractions of the canopy captured by a visible digital camera be automated? (2) what is the most appropriate method to combine visible and thermal images? and (3) what is the impact of the separation of the exposed and shaded fractions of the canopy on the mean temperature of the various fractions?

Materials and Methods

This study was carried out at the Charles Sturt University vineyard, located in Wagga Wagga, NSW, Australia (Latitude 35.05°S, Longitude 147.35°E), with an elevation of 219 m above sea level. This site has a

mean January temperature of 24.05°C and is classified as a “region IV” (hot) when using the methodology developed by Amerine and Winkler (1944). At this site the Waite index of aridity (Gentilly, 1971) is above 1 until November, indicating no requirement for irrigation, and ranges from 0.7 to 0.9 between December and March, indicating a need for irrigation in some seasons.

Vines are planted to the red cultivar Cabernet Sauvignon in a North-South direction and are trained to bilateral permanent cordons. The trellis system was originally Vertical Shoot Positioned (VSP) however the lifting wires were no longer used as part of the canopy management strategy. This lack of shoot support is partially compensated by the erect growth habit of Cabernet Sauvignon vines, but induces a canopy architecture displaying spherical leaf angle distribution, representative of a large number of commercial vineyards.

Thermal and visible images acquisition

Visible images were acquired using a digital Cyber-shot DSC–P73 camera (Sony Corporation, New York, USA) using a 2 and 3 Mega Pixel resolution. This camera uses a Charge-Coupled Device (CCD) sensor of 1/2.7” (5.37 x 4.04 mm) in size. The colour filter array is Red, Green and Blue and the storage format used was JPEG.

The thermal images were acquired using an IR SnapShot 525 (Infrared Solutions Inc., Plymouth, USA). This camera has a 20 mm lens with a 17.2° Field Of View (FOV) on the horizontal and vertical axis. This device is uncooled, handheld and uses a linear thermoelectric array to scan the focal plane of a germanium lens in the 8 to 12 µm spectral band, producing a 120 x 120 pixel image. The accuracy of the camera is 2°C or 2% of the full scale of the image.

The thermal and visible images were acquired quasi simultaneously, resting the visible image camera on the thermal camera, itself mounted on a tripod. Given the close proximity of the objectives of both cameras and the stable setup provided by the tripod, it has been assumed in the subsequent data analysis that both view angles were similar. The tripod supporting both cameras was placed such that the lens of the thermal camera was at a distance of about 2 m from the face of the grapevine. The pixel resolution of the image was 5.04 x 5.04 mm and the total area of the field of view 0.36 m².

In order to facilitate the visualisation of the thermal images, a frame was built using black polyethylene irrigation plastic tubing (approximately 600 x 500 mm). This “flag” was used to hang a wet and dry reference leaves within the field of view of both cameras as described by Jones *et al.*, (2002). The wet reference leaf was consistently placed on the left hand side of the dry reference. Both leaves were weighted down using small metal plates to maximize the leaf surface area exposed to the thermal imager and overcome the tendency of cabernet leaves to curve. Such reference leaves are typically used in the computation of relative thermal indices, not reported in this paper. Their extreme temperature regime is however of interest to this study as the reference leaves can easily be differentiated from the remainder of the canopy for analysis.

Treatment of the thermal and visible images

All visible and thermal images were treated in ENVI 4.2 (Research Systems Inc., Boulder, USA), following a 3 step methodology:

1. Separation of the exposed and shaded fractions of the canopy in the visible image using pixel classification.
2. Warping of the classified image and overlay on the thermal image.
3. Analysis of the success of the method.

Classification procedure

20 images were chosen from a large dataset and included images from mostly shaded or exposed canopy faces sampled 4 times daily. Regions of Interests (ROI) were created and saved using a consistent terminology. ROIs outlined the wet reference leaf (“Wet Ref”), the dry reference leaf (“Dry Ref”), zones of shading (“Training Shaded”) and zones of exposed leaves (“Training Exp”). The ROIs defined within the 20 visible images were compared for the separability of their spectral bands (Red, Green and Blue). Classification of the pixels within the visible images was carried out using Supervised Classification, and the “training” ROIs were used as spectral definitions. The Parallelepiped, Minimum Distance and Spectral Angle Mapper algorithms were compared for the quality of the classification outputs. The former two algorithms used variants of 2 and 3 standard deviations from the spectral band’s mean and a “user fitted” multiple value combination. The latter algorithms used variants of maximum angle values of 0.1, 0.2 and 0.3 radians. Each classified image was visually assessed against the visible image and the best classification algorithm was noted.

Warping procedure

Image to Image warping using a minimum of 4 Ground Control Points (GCPs) was used to compare the RST (Rotation, Scaling and Translation), Polynomial (1st degree) and Delaunay triangulation algorithms. Classified images were re-sampled to 120 x 120 pixels using the “Cubic Convolution” method. Visual evaluation of warped images was carried out against the original visual image and the thermal image in the area of a wet reference leaf. The use of reference leaves (wet and/or dry) is inherent to the computation of relative thermal indices noted in the introductory section of this paper. The number of classified pixels was compared on a fraction basis.

The final evaluation (Step 3 proposed above) was carried out by overlaying the classified warped images upon the thermal images and extracting the distributions of the temperatures of exposed and shaded pixels. Each fraction was compared to each other and to the mean of the combined exposed and shaded fractions. The image analysis procedure was deemed successful if a significant difference in mean temperature between the various exposure fractions or between a fraction and the combined fractions was consistently noted.

Statistical analyses

All statistical analyses were carried out using SPLUS 7 (Insightful Corp, Seattle, USA). Testing procedures included two sided paired t tests (confidence level 0.95) as well as 3 factors fixed effects ANalysis Of VAriance (ANOVA). Multiple comparisons of factor levels means were carried out using the best.fast option (including the Bonferroni, Fisher LSD, Scheffe and Tuckey procedures) at the 0.95 confidence level.

Results and Discussion

Classification procedure

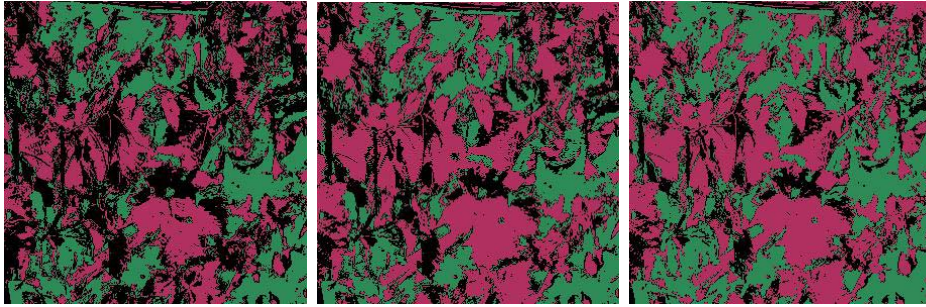
The classified visible image (see Figure 1) yielded false colour files with the same size as the original visible image but with pixels having a data value of “0” for unclassified data, “1” for exposed pixels, “2” for shaded pixels and “3” for masked pixels (reference leaves).

Visual evaluation of the classified image dataset (see Table 1) showed that the User Defined mix of standard deviation was the most appropriate method when using the Parallelepiped and Minimum Distance algorithms. The Parallelepiped algorithm was found to be the most appropriate of all the algorithms tested, in opposition with the work of Leinonen and Jones (2004). These authors however only tested the Spectral Angle Mapper and Minimum Distance algorithms. The Parallelepiped algorithm with User Defined mix of standard deviation is therefore recommended for the classification of visible images. The examination of the data did not however support the use of the Parallelepiped algorithm as an automated process, as the most appropriate User Defined mix of standard deviation is variable across images and must be defined manually by the user.

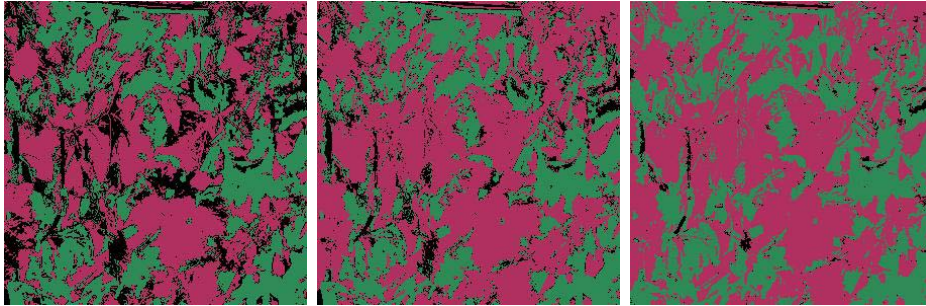
A



B



C



D

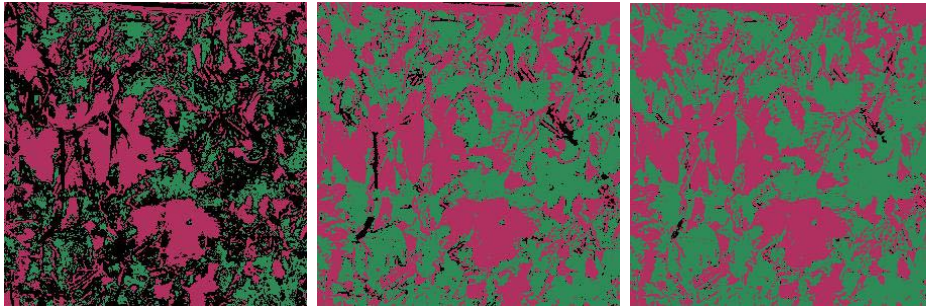


Figure 1 Classification output using ENVI 4.2 algorithms; A. Visible image of the grapevine canopy; B. “Minimum distance” algorithm, from left to right: fixed standard deviation from the mean = 2, fixed standard deviation from the mean = 3, user visual match of mixed standard deviations for the exposed and shaded fractions; C. “Parallelepiped” algorithm, from left to right: Similar to B; D. “Spectral Angle Mapper” algorithm, from left to right: Maximum angle = 0.1, 0.2 and 0.3 radians. Pink = Exposed, Green = Shade, Black = unclassified.

Table 1 Visual assessment of the effectiveness of 3 classification algorithms in ENVI 4.2 using three variants of precision levels (2 = 2 standard deviations from the mean; 0.1 = 0.1 radians maximum allowed angle from the mean). B for best achieving algorithms.

Image	Classification algorithm								
	Parallelepiped			Minimum Distance			Spectral Angle Mapper		
	2	3	User	2	3	User	0.1	0.2	0.3
1			B		B			B	
2		B				B	B		
3			B			B		B	
4			B		B			B	
5		B				B	B		
6			B		B			B	
7	B					B	B		
8			B			B		B	
9			B			B		B	
10			B			B		B	
11		B				B	B		
12		B			B			B	
13			B		B			B	
14			B			B	B		
15			B			B		B	
16			B		B			B	
17		B		B				B	
18			B			B	B		
19			B			B	B		
20			B			B		B	

Warping procedure

The 20 images classified using the Spectral Angle Mapper algorithm (0.2 radians maximum angle) were used as a standardised input data for testing the warping and re-sampling algorithms (see Figure 2). Most images warped using the Delaunay Triangulation algorithm were defined within the coordinates of the ground control points, resulting in a partially warped image. Due to this limitation, the Delaunay Triangulation algorithm was no further considered for analysis.

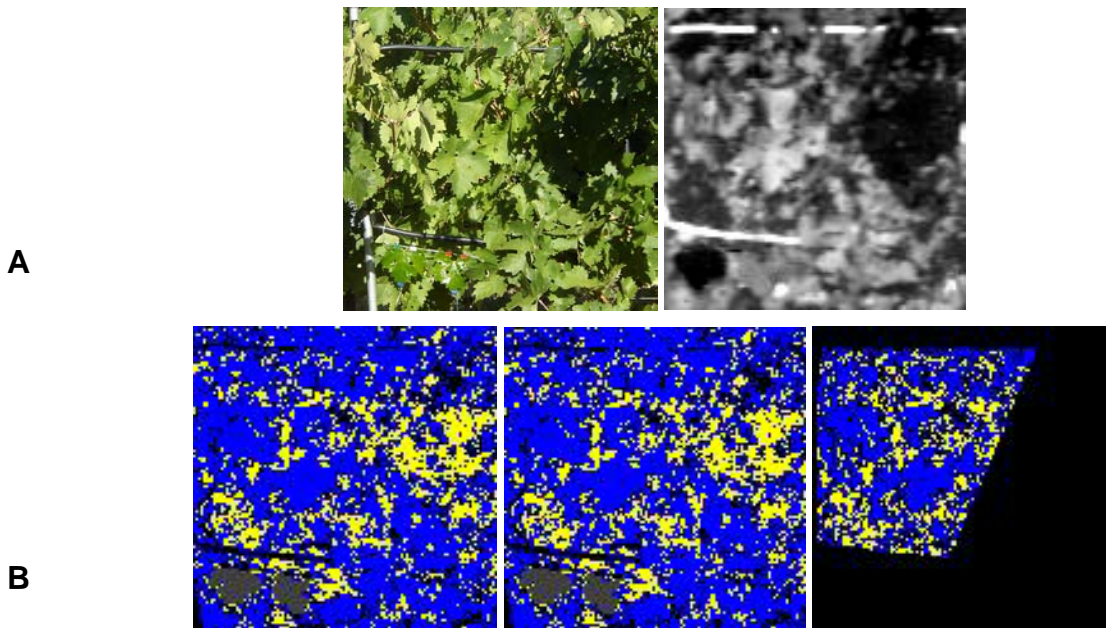


Figure 2 Warping output using ENVI 4.2 algorithms; A. Input data used for warping included a visible (left) and a thermal image (right). B. Classified and Warped output using the RST (left), Polynomial (1st degree) (centre) and Delaunay Triangulation (right) algorithms. Black, grey, yellow and blue pixels are “unclassified”, “masked”, “shaded” and “exposed” pixels respectively.

The relationship between RST and Polynomial (1st degree) warping algorithms outputs is shown in Figure 3, suggesting that both algorithms yielded similar warping output of pixels distribution per class in all but one image, represented in Figure 3 by 4 outliers (representing 4 classes per image). Furthermore a one factor ANOVA did not yield any significant difference between the RST and Polynomial factor levels. The Polynomial (1st degree) algorithm will therefore be used hereon to warp classified images for further analysis.

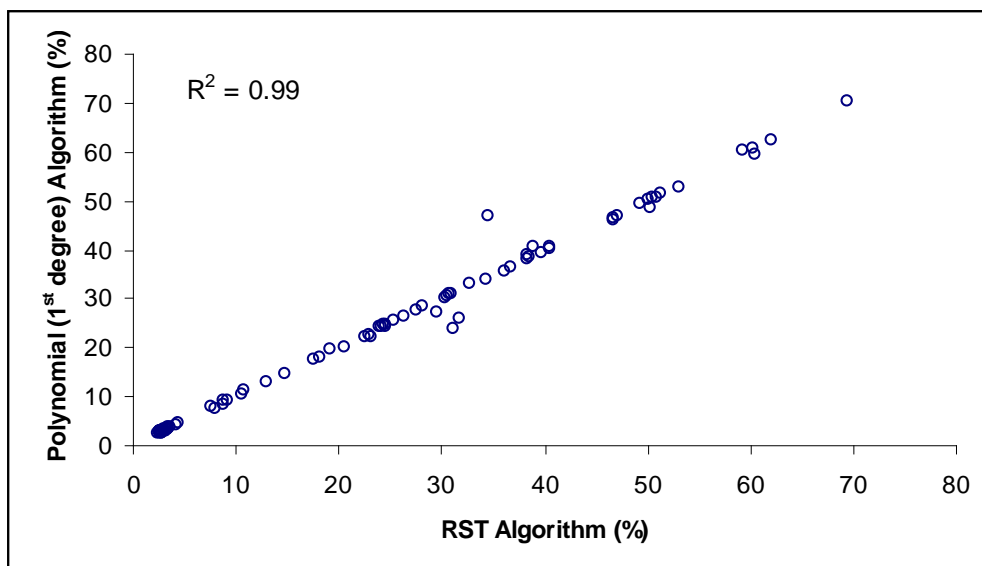


Figure 3 Relationship between the warping computations using the RST and Polynomial (1st degree) in ENVI 4.2. Values represent the percentage pixels within a full image (120 x 120 pixels resolution) belonging to one of four possible classes.

A qualitative visual assessment (see Figure 4) was carried out to identify if the warping algorithm had an impact on the fringe pixels surrounding boundary zones. The “mosaic” nature of exposed and shaded areas within the canopy may induce a significant impact on fraction temperature means and variability. The reference leaves ROIs were laid over the visible, warped visible and thermal images using warped class images.

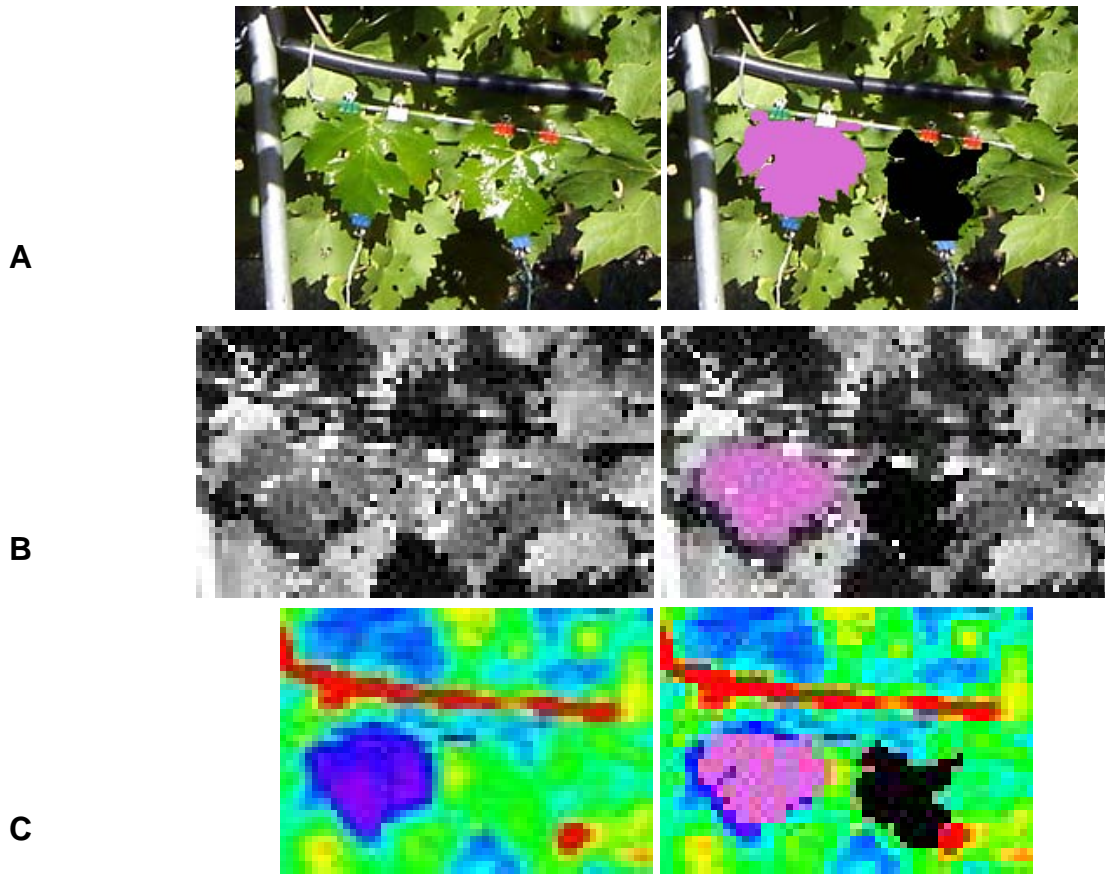


Figure 4 Visual evaluation of the capacity of the warping algorithm to identify regions of interests (pink for wet reference leaf, black for dry reference leaf). A. Visible image of reference leaves (left), showing the regions of interests defined in ENVI 4.2 (right); B. Warped and re-sampled visible image (left), showing the warped regions of interest (right); C. False colour thermal image (left), showing the warped regions of interests (right).

Figure 4 demonstrates that small areas of shading around the (left) wet reference may easily be mistaken in the thermal images as being improperly warped, unless original and warped visible images are studied concurrently. 90% of the warped reference leaves were found to overlay appropriately with the visible and thermal images. Two images were found to be difficult to interpret due to the very shaded nature of their canopies and the difficulty to delineate the reference leaves properly. It was therefore concluded that the warping of visible images was successful using the polynomial (1st degree) warping algorithm.

Thermal assessment of the exposure fractions

The methodology presented so far did not make use of the temperature thresholds defined by the wet and dry references as a mean to eliminate non-tissue material as previously proposed by Jones (1999). In this work, the vertical reference leaves were used as fixed visual references for image analysis purposes but were not representative of the spherical leaf angle distribution displayed by the canopy. The computation of the various relative indices previously described was therefore not possible using the measured data. Table 2 is a

summary of the mean temperature and standard deviation of the exposed, shaded and combined (exposed + shaded) fractions, as extracted from the thermal images using ENVI's "Post classification" tool.

Table 2 Mean temperature and standard deviation (°C) of classified fractions (exposed or shaded) and combined fractions (exposed + shaded) of grapevine canopies using ENVI 4.2

Image	Exposure fractions					
	Exposed		Shaded		Combined	
	Mean	SD	Mean	SD	Mean	SD
1	23.01	2.96	21.45	2.42	22.62	2.92
2	17.22	1.52	17.04	1.4	17.14	1.47
3	29.38	4.26	27.27	1.97	28.49	3.63
4	25.21	2.51	24.33	1.44	24.87	2.2
5	30.36	2.77	29.04	1.35	29.48	2.05
6	29	2.32	28.02	1.35	28.49	1.94
7	28.65	1.61	27.75	0.92	28.03	1.25
8	28.92	2.83	28.47	1.95	28.75	2.54
9	21.34	2.31	20.18	1.7	20.99	2.21
10	20.96	1.45	20.23	1.11	20.46	1.27
11	29.87	3.18	28.64	2.3	29.36	2.92
12	30.06	1.66	29.3	1.07	29.74	1.49
13	33.22	2.46	32.61	1.64	32.9	2.09
14	36.61	3	36.04	1.95	36.31	2.52
15	34.64	2.13	33.63	1.66	34.15	1.98
16	38.11	3.38	36.43	2.85	37.44	3.28
17	28.14	2.2	27.28	1.87	27.87	2.14
18	23.29	1.17	22.83	1.13	22.94	1.16
19	35.89	3.8	33.94	1.97	35.17	3.38
20	31.31	1.88	30.52	1.22	30.97	1.67

The shaded fractions were found to be consistently cooler than the combined fractions, themselves cooler than the exposed fractions when using t tests (confidence level 95%) on an image basis. Similarly, the standard deviation of the shaded fraction was consistently smaller than that of the combined fractions, themselves cooler than the exposed fractions.

It is therefore concluded that the use of the classification and warping algorithms was successful in separating the exposed and shaded fractions of grapevine canopies for the sample presented here. The various fractions within the field of view of the thermal imager should be considered separately when computing relative indices for irrigation scheduling purposes.

Automation of the image analysis procedure

Automation of the various steps described previously is possible in ENVI 4.2 using the embedded IDL language. Although the computation of the classification and warping algorithms is relatively simple, the methodology presented here rested upon the appropriate definition of Regions of Interest (ROIs) representative of the exposed and shaded colours of grapevine leaves at various times of day and in conditions of various levels of sun exposure. The spectral separability of the previously defined ROIs (“Training Exp” and “Training Shaded”) was computed using ENVI’s “Compute ROI separability” tool. Outputs from the “Jeffries-Matusita” and “Transformed Divergence” separability measures. separability measures, ranging from 0 to 2. Values greater than 1.9 indicate good separability (defined in ENVI 4.2 as the statistical difference between the spectral definition of two ROIs), and values smaller than 1.9 indicate that the ROIs should be edited in ENVI 4.2 for better separability. In this dataset, value were found to be consistently larger than 1.9, indicating good spectral separability of the ROIs on an image basis. These results do not however support their use as possible endmembers (pure spectral entities) or the creation of a spectral library as previously proposed by Leinonen and Jones (2004) unless the ROIs are shown to have similar value (Digital Numbers) across images on a R, G and B band basis. It was suggested by Leinonen and Jones (2004) and more recently by Moller *et al.*, (2007) that visible images may be better defined using the parameters of Hue, Saturation and Value (HSV) (Gonzalez & Woods, 2002). The Hue refers to a set palette of 360 colours and is therefore expressed as an angle. The Saturation value represents the intensity of the Hue and ranges from 0 (no colour) to 1 (very intense). Finally the Value represents the brightness of the Hue, also ranging from 0 (black) to 1 (white). The 20 visible images were HSV transformed in ENVI and both RGB AND HSV images were used to assess the impact of illumination on the previously defined ROIs. A class image of the training (Exposed and Shaded) ROIs was created and overlaid upon the RGB and HSV images. Post classification statistics were carried out on the 40 images and the digital number of each band within each image band was used as response variable in a 3 factor ANOVA including “Canopy” (factor levels “Exposed” and “Shaded”) representing the main exposure of the measured canopy face with regards to the sun’s path, “Training” (factor levels “Exposed” and “Shaded”) representing the ROIs training fractions and “Time” (factor levels “a” \approx 9am, “b” \approx 11am, “c” \approx 1pm and “d” \approx 3pm) representing the time of day the RGB (visible) image was taken. A summary of the factor effects and interactions are presented in Table 3.

Table 3 Summary of the factor effects and interactions between the training Regions of Interests (ROIs), the main exposure fraction of the canopy face measured and the time of data taking of the Red, Green and Blue bands as well as Hue, Saturation and Value of visible and HSV transformed images. Y = Factor effect observed, N = No effect and P = partial effect only.

	Bands					
	Red	Green	Blue	Hue	Saturation	Value
Canopy	N	Y	Y	Y	N	Y
Training	Y	Y	Y	Y	Y	Y
Time	P	P	P	N	N	P
Canopy:Training	N	N	Y	N	Y	N
Canopy:Time	Y	Y	Y	N	N	Y
Training:Time	N	N	Y	N	N	N
Canopy:Training:Time	N	N	Y	N	N	N

A “Training” factor effect is shown to be constantly present across the response variables, confirming the good separability of the various ROIs observed using ENVI’s “Compute ROI separability” tool. All partial “Time” factor effects reported in this analysis were due to the 9am factor level means differing from that of the 11am, 1pm and 3pm. A “Canopy” factor effect was present in 2 of 3 bands for each colour mapping technique as well as an interaction with “Time” in all RGB bands. The presence of factor effects and factor interactions for all combinations of factors indicates that the creation of a single set of endmembers for the treatment of a set of images is not appropriate using the dataset randomly selected in this work.

This work however supports the theory that a collection of endmembers can be created by splitting the RGB and HSV images into their individual bands. Artificial endmembers reflecting the various combinations of factor interactions for each image could be created according to the time of sampling, the canopy face sampled and the ROI considered for classification. Such endmember collection is likely to be site specific and would be extremely time consuming to create. It is therefore arguable that it would be more time efficient to classify RGB images using the currently proposed ROI methodology.

The factors affecting the colour composition of the RGB and HSV transformed images are considered here to be influenced by solar irradiance as well as the visible digital camera’s technical specifications (including sensor type, colour filter array and data compression). It is proposed that a standardised colour chart (composed of a combination of Saturation and Hue Digital Numbers) be included in the field of view of the visible images and that images are acquired using RAW format (free from automatic white balance and other corrections). Various calibration points of known RGB and/or HSV definition could therefore be used to stretch the data captured by the visible camera against their Digital Numbers in ENVI. If the calibration chart was to be standardised across experiments, such methodology would alleviate differences in data captured by cameras using different sensor types and colour filters.

Furthermore, the data shown in Table 3 demonstrates that the HSV methodology is relatively robust in the Saturation band and moderately robust in the Hue band across time of sampling and canopy face measured, suggesting a reduction in the number of endmember collections and a possible automation of the classification of calibrated HSV images.

Conclusions

It was shown in this work that the image analysis carried out in ENVI 4.2 was able to differentiate between exposed and shaded fractions of grapevine canopies displaying a spherical leaf angle distribution. Best results were obtained when the Parallelepiped algorithm with User Defined mix of standard deviation and the polynomial (1st degree) warping algorithm were used for the classification and warping of visible images respectively. When overlaying the warped and re-sampled classifications upon the thermal images, there were significant differences in mean temperature between the various and combined fractions. It can therefore be concluded that data manipulation (classification, warping and overlaying) is successful when carried out manually on an image basis.

The ROIs used for image classification displayed good separability but also displayed a time and canopy side factor effect. The data presented here hence do not support the possibility of a semi-automated procedure unless the factor effects noted can be reduced. It is proposed that a calibration of HSV visual data using RAW format and a standardised Hue-Saturation chart placed in the field of view of the image be used to facilitate the automation of the classification procedure in future work.

Acknowledgements

The authors express their gratitude to CSIRO Sustainable Ecosystems and CSIRO Plant Industry for the funding of the PhD project leading to this publication. The authors express their gratitude to the CRC for Viticulture for its support and financial contribution to the project.

References

- Amerine, M.A., and A.J. Winkler. 1944. Composition and quality of musts and wines of California grapes. *Hilgardia*. 15:493-675.
- Bhuiyan, C. 2004. Various drought indices for monitoring drought condition in Aravalli terrain of India. *In XXth ISPRS Congress, Geo-Imagery Bridging Continents Istanbul, Turkey*.
- Blad, B.L., B.R. Gardner, D.C. Watts and N.J. Rosenberg. 1981. Remote sensing of crop moisture status. *Remote Sensing Quarterly*. 3:4-20.
- Cohen, Y., V. Alchanatis, M. Meron, Y. Saranga and J. Tsipris. 2005. Estimation of leaf water potential by thermal imagery and spatial analysis. *Journal of Experimental Botany*. 56:1843-1852.
- Fuchs, M. 1990. Infrared measurement of canopy temperature and detection of plant water stress. *Theoretical and applied climatology*. 42:253-261.
- Fuentes, S., J.P. Conroy, G. Kelley, G. Rogers and M. Collins. 2005. Use of infrared thermography to assess spatial and temporal variability of stomatal conductance of grapevines under partial rootzone drying: An irrigation scheduling application. *In VIIth International Symposium on Grapevine Physiology and Biotechnology, Davies, California, USA*.
- Gentilly, J. (Ed.). 1971. *Climates of Australia and New Zealand*. (Vol. 13). Elsevier, Amsterdam.
- Gonzalez, R., and R.E. Woods. 2002. *Digital Image Processing (2nd ed.)*, Prentice Hall Press.

- Guisard, Y. 2008. Crop canopy temperature as indicator of water stress: Application to grapevines. PhD Thesis. Charles Sturt University, Faculty of Science, School of Agricultural and Wine Sciences, Wagga Wagga, Australia.
- Hiler, E.A., T.A. Howell, R.B. Lewis and R.P. Boos. 1974. Irrigation timing by the Stress Day Index method. *Transactions of the ASAE*. 393-398.
- Idso, S.B., R.D. Jackson, P.J. Pinter Jr; and R.J. Reginato. 1981. Normalising the stress degree day parameter for environmental variability. *Agricultural meteorology*. 24:45-55.
- Idso, S.B., R.D. Jackson, and R.J. Reginato. 1977. Remote sensing for agricultural water management and crop yield prediction. *Agricultural Water Management*. 1:299-310.
- Jones, H.G. 1999. Use of infrared thermometry for estimation of stomatal conductance as a possible aid to irrigation scheduling. *Agricultural and Forest Meteorology*. 95:139-149.
- Jones, H.G. 2004. Irrigation scheduling: advantages and pitfalls of plant based methods. *Journal of Experimental Botany*. 55:2427-2436.
- Jones, H.G., M. Stoll, T. Santos and C. de Sousa. 2002. Use of infrared themography for monitoring stomatal closure in the field: application to grapevine. *Journal of Experimental Botany*. 53:2249-2260.
- Kogan, F.N. 1995. Application of vegetation index and brightness temperature for drought detection. *Advances in Space Research*. 15:91-100.
- Leinonen, L. and H.G. Jones. 2004. Combining thermal and visible imagery for estimating canopy temperature and identifying plant stress. *Journal of Experimental Botany*. 55:1423-1431.
- Moller, M., V. Alchanatis, Y. Cohen, M. Meron, J. Tsipris, A. Naor, V. Ostrovsky, M. Sprintsin and S. Cohen. 2007. Use of thermal and visible imagery for estimating crop water status of irrigated grapevine. *Journal of Experimental Botany*. 58:827-838.
- Moran, M.S., T.R. Clarke, M. Inoue and A. Vidal. 1994. Estimating crop water deficit using the relation between surface air temperature and spectral vegetation index. *Remote Sensing of Environment*. 49:246-263.
- Rodriguez, D., V.O.Sadras, L.K.Christensen, and R. Belford. 2005. Spatial assessment of the physiological status of wheat crops as affected by water and nitrogen supply using infrared thermal imagery. *Australian Journal of Agricultural Research*. 56:983-993.
- Singh, R. P., S. Roy, and F.N. Kogan. 2003. Vegetation and temperature condition indices from NOAA AVHRR data for drought monitoring over India. *International Journal of Remote Sensing*. 24:4393-4402.
- Stoll, M., and H.G. Jones. 2005. Infrared thermography as a viable tool for monitoring plant stress. *In XIVth International GESCO Symposium, Geisenheim, Germany*.
- Tanner, C. B. 1963. Plant temperatures. *Agronomy Journal*. 55:210-211.